AN EXPERIMENTAL OVERVIEW OF MESON SPECTROSCOPY DATA

Curtis A. Meyer
Carnegie Mellon University, Pittsburgh, PA 15213

Abstract

In this article, I will provide an introduction to the field of experimental meson spectroscopy. I will start with a brief overview of how we classify mesons, and determine which mesons are which. I will then give a summary of how we extract mesons properties from data, and finally overview what the current issues are in the field.

INTRODUCTION

This article is meant as an introduction to the field of meson spectroscopy, it is not intended to be a comprehensive review of the subject. I have divided this article into four parts. Initially, I will identify what mesons are, and how we classify them. In particular, their nonet structure and how we can use mass, width and decay patterns to assign them. Next, I will review partial wave analyses, and how we use this information to extract the quantum numbers of the mesons. I will then discuss what the current issues in meson spectroscopy are, and how these issues can help us understand non-perturbative QCD. Finally, I will discuss the issues which we can address using an upgraded CEBAF with 10 to 12 GeV photons.

MESON SPECTROSCOPY

The field of light–quark meson spectroscopy studies mesons made of u, d and s quarks. In the quark model, a meson is built from a quark and an antiquark. Given three flavors of quarks, there are nine different quark combinations. SU(3) flavor breaks these into an octet and a singlet. The physical isoscalar states are normally mixtures of the singlet state, $| 1 >$, and the isoscalar octet state, $| 8 >$, (see diagram below). For the pseudo–scalar nonet, the mixing angle is measured to be $-20°$. For $\theta \approx 36°$, the two isoscalar states become $| s\bar{s} >$ and $| \frac{1}{\sqrt{2}}(u\bar{u} + d\bar{d} >$. This is known

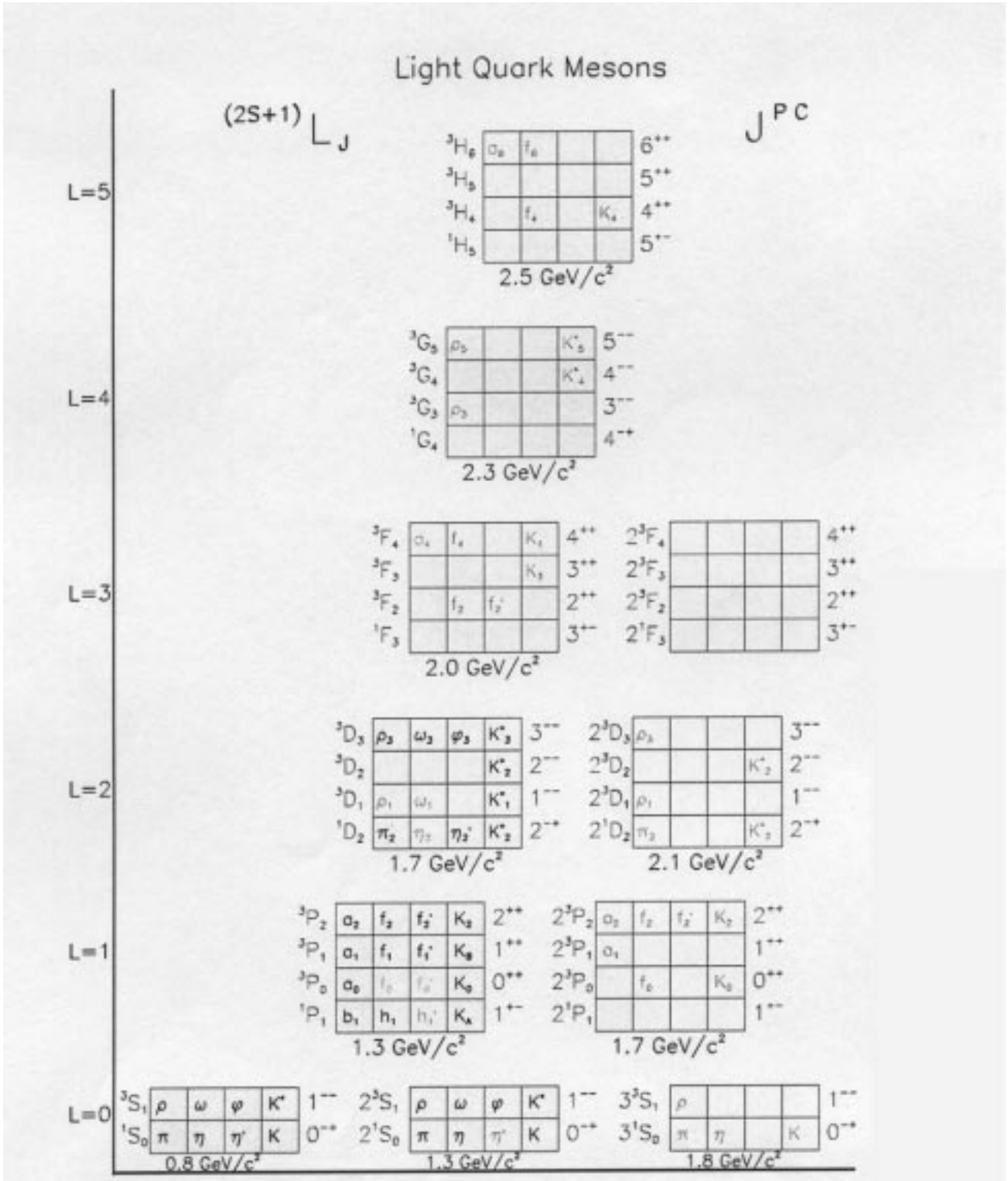

Figure 1: Spectrum of Mesons expected in the Quark–Model

as *ideal mixing*; both the vector and tensor meson are nearly ideally mixed. In fact, the only nonet known to be far from ideal mixing is the pseudo–scalars.

$$\begin{array}{ccc} K^\circ & K^+ & \\ \pi^- & \pi^\circ & \pi^+ \\ K^- & \bar{K}^\circ & \end{array} \qquad \begin{array}{ccc} d\bar{u} & \frac{1}{\sqrt{2}}(d\bar{d} - u\bar{u}) & u\bar{d} \\ s\bar{u} & & s\bar{d} \end{array} \qquad \begin{bmatrix} \eta \\ \eta' \end{bmatrix} = \begin{bmatrix} \cos\theta & \sin\theta \\ \sin\theta & \cos\theta \end{bmatrix} \begin{bmatrix} |8> \\ |1> \end{bmatrix}$$

$$\eta\,\eta' \qquad |8> = \frac{1}{\sqrt{6}}(u\bar{u} + d\bar{d} - 2s\bar{s}) \qquad |1> = \frac{1}{\sqrt{3}}(u\bar{u} + d\bar{d} + s\bar{s})$$

A $\bar{q}q$ system can have the two spin $\frac{1}{2}$ quarks in either a spin singlet, $S = 0$, or a spin triplet, $S = 1$ state. In addition, there is a relative orbital angular momentum L between the $q\bar{q}$ pair and a total spin J of the system. Finally, there are radial excitations, n, of the $q\bar{q}$ system. A particular nonet is then described in spectroscopic notation as $n^{2s+1}L_J$. In this notation, the pseudo-scalar mesons, (π, K, η and η'), are 1^1S_0 mesons, and the vectors, (ρ, K^*, ω and ϕ), 1^3S_1 mesons. Because most of the processes of interest are purely strong interactions, we denote the mesons in terms of the conserved quantum numbers, $(I^G)J^{PC}$: isospin ,I; G–parity, G; total spin, J; parity, P; and C–parity, C, . For a $\bar{q}q$ system, $P = -(-1)^{(L)}$, $C = (-1)^{(L+S)}$ and $G = (-1)^{(L+S+I)}$. A nice description is given in reference [1].

This leads to the expected spectrum of nonets shown schematically in Figure 1. The states labeled in black are reasonably well established, while those labeled in gray either need confirmation, or the assignment is not certain. The empty boxes indicate states which are not known. The mass listed below each box are taken from reference [2]. They are the estimated mass of the states containing mostly u and d quarks.

In order to uniquely identify that a state belongs to a particular nonet, it is necessary to look at several properties of the state. Table 1 lists the tensor mesons, $J^{PC} = 2^{++}$ along with their masses, widths, and known two pseudo–scalar decay modes. Given a series of mesons which we believe belong to the same nonet, we can use the mass relation in equation 1 to arrive at a mixing angle for the nonet.

	Mass	Width	$\pi\pi$	$K\bar{K}$	$\eta\eta$	$\pi\eta$	$\pi\eta'$	$K\bar{K}$	$K\pi$	$K\eta$
a_2	1318	104				15%	0.5%	5%		
f_2	1275	186	85%	5%	0.5%					
f_2'	1525	76	1%	10%	89%					
$K_2^{*\pm}$	1425	100							50%	0.1%
$K_2^{*\circ}$	1432	109								

Table 1: The tensor, ($J^{PC} = 2^{++}$), mesons and the decay rates into pairs of pseudo–scalar mesons.

$$\tan^2\theta \;=\; \frac{3m(f_2') - 4m(K_2) + m(a_2)}{4m(K_2) - m(a_2) - 3m(f_2)} \qquad (1)$$

Applying this to the tensor mesons, we find $\theta_2 = 26°$. This mixing angle can then be used to predict decay strengths into pairs of pseudo–scalar mesons. Correcting

the decay rates by the available phase space as well as an L dependent angular momentum factor, we can then express the decays for a given nonet in terms of one decay constant. A nice description of this procedure is given in reference [3], where the authors also include a possible glueball admixture in addition to the nonet mixing angle. This procedure works extremely well for the tensor mesons.

IDENTIFICATION OF MESONS

Mesons have been studied in several different production mechanisms which are cartooned in Figure 2. In the left–most plot, diffraction is sketched. This process involves the exchange of a particle with vacuum quantum numbers, 0^{++}, and is often called pomeron exchange. We do not really understand what the pomeron is, but many models try to explain it as two–gluon exchange. A related process, double–diffractive production in which two pomerons are exchanged is believed to be a glue–rich channel, and a good source of glueballs. The pomeron processes dominate at high energy. The left center picture shows t–channel meson exchange. Here, we replace the M with a π, ρ, ω,.... This process has a different t dependence, and if the exchanged particle is charged, this can be differentiated from the pomeron exchange. These processes are more important at lower beam energy, however for 8 to 12 GeV beams, we would expect both to be important. The right center process in Figure 2 is what I call annihilation. In this, I consider $\bar{p}p$ and J/ψ annihilations. In both these, the quantum numbers of the initial state are known, and one looks for a system X recoiling against a spectator meson **m**. The $\bar{p}p$ system at rest is a very good source of scalar mesons, and both of these reactions are considered to be glue–rich. Finally, in the right diagram are what I consider to be s–channel processes. Here two particles fuse to form the final state X, either e^+e^- or $\gamma\gamma$. In the former, we only produce vector mesons, 1^- states, while in the latter $C = +1$ states are produced.

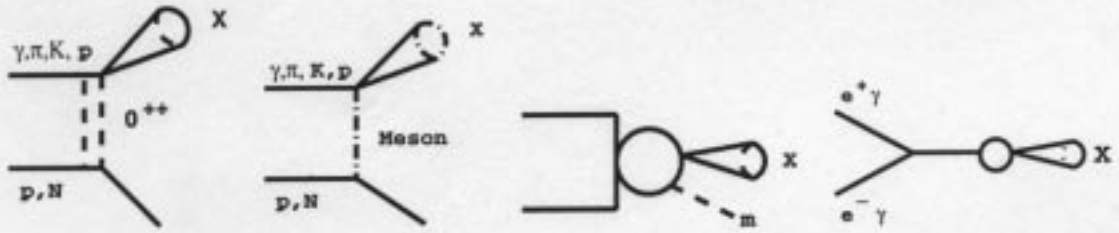

Figure 2: Production mechanisms for producing mesons

Depending on the beam and mechanism, different types of mesons are more likely to be produced. Kaon beams are a good way to produce both the excited Kaons, as well as the mostly $s\bar{s}$ mesons. Certain reactions such as J/ψ decays, $p\bar{p}$ annihilations and double pomeron exchange are considered to be glue–rich. Other reactions such as $\gamma\gamma$ and e^+e^- are felt to be glue–poor environments. $\bar{p}p$ annihilations at rest favor production of scalar mesons, and $\bar{s}s$ states tend to be weakly produced. The bottom line is that looking at the different production mechanisms of a meson can also yield information on its constituents.

PARTIAL WAVE ANALYSIS

In order to identify the J^{PC} quantum numbers of a meson, it is necessary to perform a partial wave analysis. In the simplest terms, a partial wave analysis attempts to fit a decay angular distribution, which in turn depends on the production mechanism, the spin and parity of the resonance, the spin and parity of any daughter resonances, and any relative orbital angular momenta. In addition, the analysis needs to establish phase motion of the particle consistent with a resonance.

In the case of either J/ψ decay or $\bar{p}p$ annihilation at rest the analyses are quite similar. The system starts in a well defined state, ($(I^G)J^{PC}$ are known). If we then consider a process such as $\bar{p}p \to abc$, we assume that this can be described in terms of the isobar model [4], which leads to the chain shown in eqn. 2.

$$\underbrace{I}_{J_0} \to \overbrace{\underbrace{A}_{J_A}\ \underbrace{c}_{J_c}}^{L_A} \to \overbrace{\underbrace{a}_{J_a}\ \underbrace{b}_{J_b}}^{L_a} c \tag{2}$$

The angular distributions, $\mathcal{Z}(J_0; J_A, J_a, J_b, \cdots; L_A, L_a)$, can be described in terms of the helicity formalism, (see reference [5] for a description with good examples). The angular distribution is a function of all the spins and angular momenta in the problem, but in fact may not be unique. I.e. two or more sets of spins and angular momenta may yield the same distributions. In addition to the angular distributions, there are also dynamics which are described by production and resonance parameters, $\mathcal{F}(m_A, \Gamma_A, m_a, m_b, m_c, \cdots)$. In the case of a single resonance whose width is much smaller than its mass, this function would be a Breit–Wigner. In reality, one has many resonances with possibly unknown production mechanisms and and several different decay modes. One way to handle this is in the K–matrix formalism, which is particularly powerful when more than one final state of a resonance have been measured in the same experiment. A good article on this can be found in reference [6].

In the case of a three–body final state, the analysis is normally carried out in the framework of a Dalitz plot. Figure 3 shows the Dalitz plot for the process $\bar{p}n \to \eta\pi^\circ\pi^-$ at rest, (these data are taken from reference [7]). The prominent diagonal band is the $\rho^-(770)$ recoiling against a spectator η. There is also a horizontal band corresponding to the $a_2^\circ(1320)$ against a spectator π^- and a vertical band corresponding to the $a_2^-(1320)$ recoiling against a spectator π°. The data are fit identifying a complex amplitude, $\mathcal{A} = \mathcal{Z} \cdot \mathcal{F}$, for each possible resonance. Those from the same initial state are added coherently, and then squared to yield an estimated weight for each bin in the Dalitz plot. The parameters of the complex amplitudes, as well as their relative strengths and phases are varied to minimize a χ^2 difference between the data and the fit.

Only fitting with the amplitudes listed above yields a χ^2 per degree of freedom of 2.69. The difference between the fit and the data are shown in Figure 3**b**. The structure in this plot indicates that there is something missing in the fit. Adding a resonance in the $\eta\pi$ P–wave to the mix reduces the χ^2 per degree of freedom down to 1.29 and produces the difference plots shown in Figure 3**c**. The differences are now essentially statistical in nature.

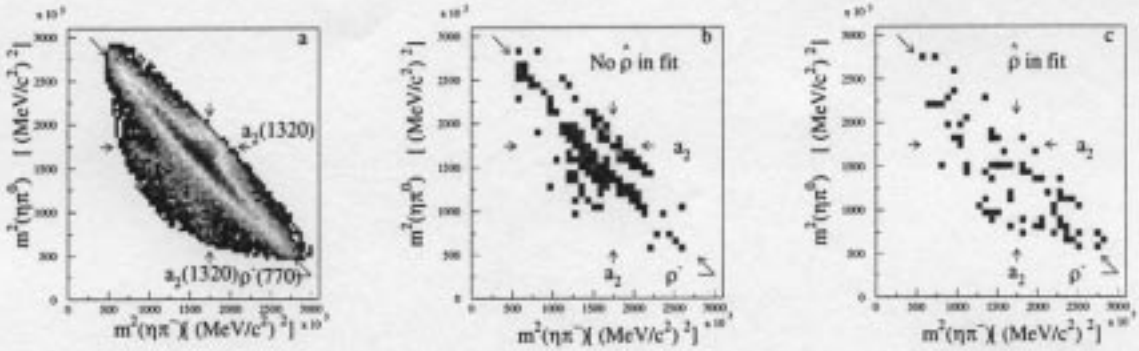

Figure 3: **a** The Dalitz plot for $\bar{p}n \to \eta\pi^{\circ}\pi^{-}$. The χ^2 difference between fit and data without the $\hat{\rho}$, (**b**) and with the $\hat{\rho}$, (**c**).

In the case of either the diffractive production or the t–channel exchange, the partial wave analysis is done in a somewhat different way. The underlying assumption here is that the amplitudes can be broken in to two or more incoherent sets. These essentially correspond to spin–flip and spin–non-flip amplitudes [8]. In these procedures, only the X system of Figure 2 is treated. The data are binned according to the mass of X, and with a series of functions which only describes the angular distributions of the final state particles are fit two each bin. From these fits, one extracts the intensity and phase of each partial wave as a function of mass. Figure 4 shows the results from one of these fits taken from reference [9]. Figure 4**a** shows m_X, in this case $\pi^+\pi^-\pi^-$. Figures 4**b** and **c** show the fit intensity in the 1^{++} and 2^{-+} partial waves. These results are then fit two the assumption of resonances in the partial waves. Here explaining the relative phase differences is key to extracting the resonance parameters.

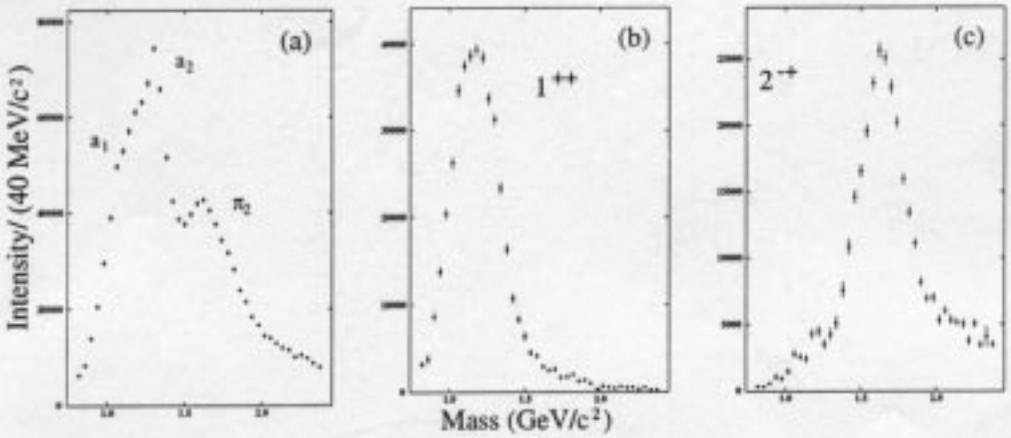

Figure 4: Fit results for $\pi^- p \to \pi^+\pi^-\pi^- n$ taken from reference [9].

Finally, when fitting the resonance parameters, it is important to cite the

T–matrix poles rather than the *simple Breit–Wigner* masses and widths. The latter can be severely distorted by the production method, decay thresholds, and other resonances, while the former have all these effects built in and are a better representation of the actual resonance.

ISSUES IN SPECTROSCOPY

Given the issues in identifying and cataloging mesons, we now come to the question of what are the interesting topics in meson spectroscopy? Figure 1 of reference [10] shows a modified view of Figure 1. It shows not only the normal mesons, but also expectations for glueballs, hybrid mesons, and where several meson–meson molecular thresholds lie. See reference [11] for a more detailed description of these states and their properties. I will only mention that all models of non–perturbative QCD as well as lattice calculations predict that these states exist. While many of these have the same quantum numbers as ordinary mesons, and are likely to be mixed, there are several that have exotic, or non–$q\bar{q}$ quantum numbers. In fact there is recent evidence of such states [7], [9], [12].

Even in the few situations where we have identified a number of states, the identification of a particular state is often hindered by its observation in only one production mechanism, and only a very small number of decay modes. As an example, we will consider the 2^{++} and J^{--} states.

Of all the higher mass mesons, there are more known 2^{++} states than anything else. In Figure 5 are listed the known 2^{++} mesons from reference [13]. The bars indicate the expected location of the first radial states, the ${}^3F_2$ states and the glueball. Also indicated are some of the ${}^3F_4$ states which are expected to have similar masses to the ${}^3F_2$ states. The f_2 states have the same quantum numbers as the expected 2^{++} glueball. Finally, we give the known decay modes from largest to smallest. Even with all these states, there are difficulties in assigning them. In my opinion, the $f_2(1565)$ and $f_2(1640)$ are probably the same state, just seen in different production mechanisms. One would then like to assign the $f_2(1810)$ as the radial excitation of the $f_2'(1525)$. Unfortunately the $K\bar{K}$ mode is probably too small. The $f_2(1950)$ is also a candidate for this state, but there is also speculation that this broad state has a large glueball content [14]. The $f_J(2220)$ or ξ is also a glueball candidate because of its very narrow width, and large rate in radiative J/ψ decays [15]. Finally, there are several higher mass states that have only been observed in one or two decay modes. In order to untangle what is going on we need to know more about the decay patterns of these states. In particular, unraveling the 4π modes such as:

$$f_2 \to (f_2(1270))(\pi\pi)_S \to (\pi\pi)(\pi\pi) \qquad f_2 \to (f_2'(1525))(\pi\pi)_S \to (K\bar{K})(\pi\pi)$$
$$f_2 \to (\pi_2(1670))\pi \to (f_2(1270)\pi)\pi \to (\pi\pi)\pi\pi \qquad f_2 \to (a_2(1320))\pi \to (\rho\pi)\pi \to (\pi\pi)\pi\pi$$

could lead to insight on the nature of these states. Many of the expected decay patterns have been computed in the ${}^3P_0$ model [16]. Understanding what the states are and how the 2^{++} glueball has mixed into these states is important information that can be extracted from these states.

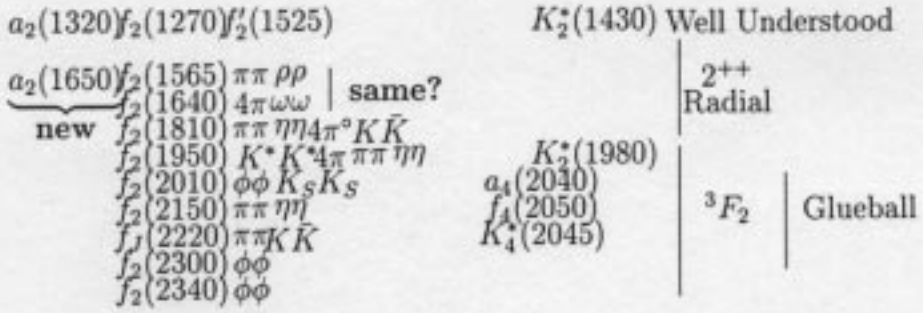

Figure 5: The 2^{++} mesons as of reference [13].

Next we examine the J^{--} mesons. Figure 6 shows the currently known states, as well as expected missing states, (inside the box). In addition to the meson states, a $J^{PC} = 1^{--}$ hybrid nonet is expected around a mass of 1800 MeV/c^2. Given the proximity of the $^3D_1$ and both 2^3S_1 and 3^3S_1 states, strong mixing cannot be excluded. Also, recent observations of the $\rho(1450)$ and $\omega(1420)$ indicate that they have large rates to the ground state vector plus $(\pi\pi)_S$ [17], [18]. This leads one to speculate that a similar decay should be present for the $\phi(1680)$. These decays do not appear important for the $\rho(1700)$ and the $\omega(1600)$. It is these latter states which people speculate are strongly mixed with the hybrid nonet. Unfortunately, only detailed studies of the decay patters will allow us to unravel this. Reference [16] calculates the various rates for both the $^3D_1$ and hybrid ρ. Detailed comparison with currently emerging results may yield new insights on this problem. The bottom line is that we do not understand these states particularly well.

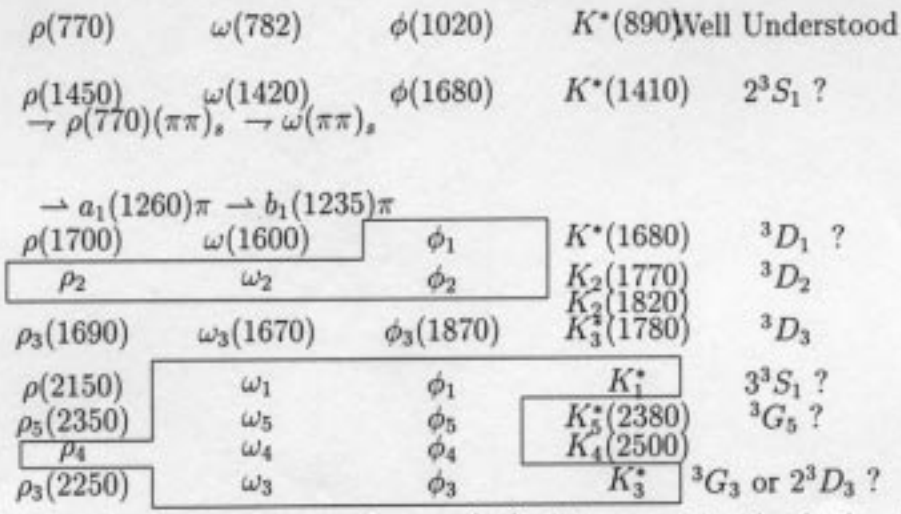

Figure 6: The J^{--} states from reference [13]. The states inside the box have not been observed.

Our understanding of non-perturbative QCD could be significantly advanced by being able to experimentally identify the orbital and radial excitations of mesons, and their likely mixings. More significantly, finding the expected gluonic states,

(hybrids and glueballs) and understanding their mixings with the normal $q\bar{q}$ states would expand our understanding of just how glue behaves. Several talks at this workshop have addressed the role of photo production that could be exploited at CEBAF. Reference [20] discusses the $s\bar{s}$ spectrum, which takes advantage of the fact that there is a significant $s\bar{s}$ content in the photon. Reference [19] discusses why photo production is expected to be a good place to find hybrid mesons, and which ones would be most easily seen. Finally, reference [10] discusses the *Hall D* project to build a state of the art detector whose main goal would be to study meson spectroscopy.

References

[1] F. E. Close, **An Introduction to Quarks and Partons**, (1979), Academic Press, Harcourt Brace Jovanovich, Publishers.

[2] Stephen Godfrey and Nathan Isgur, Phys. Rev. **D32**, 189, (1985).

[3] Claude Amsler and Frank E. Close, Phys. Rev. **D53**, 295, (1995).

[4] D. Herndon, P. Söding and R. J. Cashmore, Phys. Rev. **D11**, 3165, (1975).

[5] C. Amsler and J. C. Bizot, Comp. Phys. Comm. **30**, 21, (1983).

[6] S. U. Chung, J. Brose, R. Hackmann, E. Klempt, S. Spanier and C. Strassburger, Annalen Phys. **4**, 404, (1995).

[7] The Crystal Barrel Collaboration, A. Abele *et al.*, Phys. Lett. **B423**, 175, (1998).

[8] S. U. Chung and T. L. Trueman, Phys. Rev. **D11**, 633, (1975).

[9] G. Adams, *et al.*, **Observation of a new $J^{PC} = 1^{-+}$ exotic state in the reaction $\pi^- p \to \pi^+\pi^-\pi^-$ at 19 GeV/c**. Submitted for publication in Phys. Rev. Lett., (1998).

[10] Alex R. Dzierba, these conference proceedings.

[11] Eric Swanson, these conference proceedings.

[12] D. R. Thompson, *et al.*, Phys. Rev. Lett. **79**, 1630, (1997).

[13] C. Caso, *et al.*, The Particle Data Group, The European Physical Journal **C3**, 1, (1998).

[14] D. V. Bugg and B. S. Zou, Phts. Lett. **B396**, 295, (1997).

[15] J. Z. Bai, *et al.*, The BES Collaboration, Phys. Rev. Lett. **76**, 3502, (1996).

[16] T. barnes, F. E. Close, P. R. Page and E. S. Swanson, Phys. Rev. **D55**, 4157, (1997).

[17] U. Thoma, **Antiproton–Nucleon Annihilation at Rest into Five Pions**. Too be published in the Proceedings of Hadron '97.

[18] R. McCrady, **Study of $\bar{p}p$ annihilations at rest into $\omega\pi^+\pi^-\pi^\circ$**. Too be published in the Proceedings of Hadron '97.

[19] T. Barnes, these conference proceedings.

[20] D. Tedeschi, these conference proceedings.